Marine Geology 428 (2020) 106279

Contents lists available at ScienceDirect

Marine Geology

journal homepage: www.elsevier.com/locate/margo

Sedimentary transition of the Yangtze subaqueous delta during the past century: Inspiration for delta response to future decline of sediment supply

Qing Zhan[a,b], Maotian Li[b,*], Xiaoqiang Liu[b], Jing Chen[b,*], Zhongyuan Chen[b]

[a] Shanghai Institute of Geological Survey, Shanghai 200072, China
[b] State Key Laboratory of Estuarine and Coastal Research, East China Normal University, Shanghai 200241, China

ARTICLE INFO

Keywords:
delta progradation
delta retrogradation
erosion
sediment supply decline
sedimentary transition

ABSTRACT

How the Yangtze delta responds to riverine sediment decline has become a hot research topic and an urgent issue to be addressed, especially after the impoundment of the Three Gorges Dam in 2003. This study investigated sedimentary features through the sediment granularity of surficial samples and short cores over the entire Yangtze subaqueous delta, aiming to better understand the spatial response of the subaqueous delta to sediment supply decline and local hydrodynamic adjustment of the estuary. The results show that four sedimentary zones of estuarine sand bar (Zone I), prodelta (Zone II), delta-shelf transition zone (Zone III) and residual sand (Zone IV) are distributed from the estuary to the shelf, characterised by first fining from zone I to zone II, and then coarsening from zone II to zone IV on grain size of surficial sediments. In the past few hundred years, the subaqueous delta has been generally prograded seaward following this sedimentary system spatially, manifested by generally fining upwards in the cores of the main subaqueous delta. However, sediment coarsening occurs on the top of the cores in the delta-shelf transition zone (Zone III), implying a recent retrogradation process. Based on the results of ^{210}Pb and ^{137}Cs, the sedimentary transition from progradation to retrogradation occurred since 1950s and was intensified after 1980s in the north part of Zone III, mainly caused by channel shrinking of the North Branch and riverine sediment decline. Comparatively, such a sedimentary transition is not significant in the south part of Zone III. But it is worth noting that surficial coarsening in the core (of the south part of Zone III) is probably related to drastic sediment decline since 2003 when the Three-Gorges Dam closed, which means that the Yangtze subaqueous delta has probably been in a full sedimentary transition. The sedimentary transition of the north subaqueous delta can provide an insightful reference for the sedimentary response of the Yangtze delta to further decline of sediment supply in the future.

1. Introduction

Since the global sea level stabilized at 7000 years BP., large river deltas have begun to develop and prograde continuously to the sea (Stanley and Warne, 1994; Chen et al., 2000). The accumulated deltas provided superior geographical conditions for the prosperity of the Neolithic civilization (Chen et al., 2005; Zong et al., 2007; Carozza et al., 2012). Since then, these deltas have been densely populated and economically developed all over the world. However, intensive human activities, such as dam construction in these basins, have caused a sharp decline of riverine sediment supply globally in the past century (Syvitski et al., 2009; Giosan et al., 2014). Many mega-deltas are in overall erosion or facing the risk of erosion, such as those of the Nile, Mississippi, and Yellow Rivers (Chu et al., 2006; Blum and Roberts, 2009; Besset et al., 2019; Maloney et al., 2019; Nienhuis et al., 2020). The Yangtze delta has been also listed as a high-risk region without exception (Wang et al., 2018; Besset et al., 2019).

The Yangtze River has three main hydrological stations with continuous flux records of water and sediment during the past century, which provides the possibility for researching basin-scale hydrological response and further delta-scale geomorphological response to climate change and human activities (Yang et al., 2011; Chen et al., 2014). It is an indisputable fact that sediment loads have continuously declined due to the increasing reservoir capacity of the Yangtze basin since 1950s (Yang et al., 2011, 2014). How the Yangtze delta responds to riverine sediment decline has become a hot topic and an urgent issue to be answered. Many recent studies have found that estuarine sand bars and tidal flats are still in accretion, and erosion seems to occur only at the outer part of the subaqueous delta, despite of decreasing sediment supply from the Yangtze River (Yang et al., 2011; Dai et al., 2014). Luo

* Corresponding authors.
E-mail addresses: mtli@sklec.ecnu.edu.cn (M. Li), jchen@geo.ecnu.edu.cn (J. Chen).

https://doi.org/10.1016/j.margeo.2020.106279
Received 7 April 2020; Received in revised form 18 June 2020; Accepted 20 June 2020
Available online 25 June 2020
0025-3227/

et al. (2012, 2017) also found that surficial sediment was coarsening between the Yangtze estuary and shelf due to the recent decline of sediment supply, through comparing sediment granularity collected in the two surveys separated by 30 years. The knowledge obtained from these studies is based on direct comparisons of surficial sediments or bathymetry from sea charts among multiple years, lacking continuous sedimentary records. Besides, the study areas in the most studies do not cover the entire subaqueous delta, which might limit the perception of delta response to basin-scale activities. For example, recent studies have shown that estuarine activities such as large channel projects might have a greater impact on local geomorphological change than basin-scale activities (Dai et al., 2016; Zhang et al., 2019). Therefore, only when the samples cover the entire subaqueous delta spatially and are continuous temporally, can the delta response to basin-scale activities be viewed objectively.

This study aims to evaluate deltaic sedimentary changes during the past few centuries, through the sediment granularity of surficial samples and short cores throughout the Yangtze subaqueous delta. This can help in better understanding the spatial response of the subaqueous delta to the decline of riverine sediment supply.

2. Materials and methods

Totally 1076 surficial samples and 42 cores were taken throughout the Yangtze subaqueous delta in 2012. In addition, 23 surficial samples and one core (YZE) were collected from Luo et al. (2012) and Chen et al. (2014) respectively for the purpose of this study. Detailed information is shown in Fig. 1 and Table 1.

The radiocarbon ages (AMS^{14}C) of 6 shell samples from the 5 cores were measured by Beta Analytic using accelerator mass spectrometry (Table 2). All the AMS^{14}C ages were calibrated using the Calib 7.1 program (Stuiver et al., 2015). In which, the ΔR value (135 ± 42) was adopted for the Marine13 calibration curve reported by Yoneda et al. (2007). The calibrated ages at 1σ with probabilities > 0.8 were adopted in this study.

1075 samples were taken at 2–4 cm intervals from the 14 cores for measurements of ^{210}Pb and ^{137}Cs (Fig. 1; Table 1). All samples were analyzed by the Nanjing Institute of Geography and Limnology, Chinese Academy of Sciences. 10 g sediments of each sample were dried for the planer detector, in which 5 g were ground, homogenized, and stored in the sealed plastic vessels for the well detector. These samples were left for at least 2 weeks to establish a radioactive equilibrium between ^{226}Ra and ^{222}Rn. Then specific gamma rays of ^{210}Pb (46.5 keV) and ^{214}Pb (351.9 keV) were measured using a model GWL-120-15 well germanium detector and model jr2.0 multiple channel analyser. Excess ^{210}Pb activities were calculated by subtracting ^{214}Pb activities on the assumption that the supported ^{210}Pb from ^{226}Ra is equal to ^{214}Pb. The average sedimentation rate of the core was calculated from the slope of the logarithm regression line of excess ^{210}Pb against depth and radioactive decay constant (0.03114 yr^{-1}) according to the Constant Initial Concentration (CIC) model. ^{137}Cs was measured by gamma rays spectrometry based on photon energies at 661.62 keV and its initial emergence upwards in the core was believed as the time of 1950s(Huh and Su, 1999).

A total of 2106 samples were taken at 2–6 cm intervals from the 42 cores (Table 1). All these samples and 1076 surficial samples were analyzed for grain size in the State Key Laboratory of Estuarine and Coastal Research, using a Beckman Coulter Laser Diffraction Particle Size Analyzer (LS13320). Furthermore, we collected grain size data of 23 surficial samples in the Yangtze subaqueous delta and its adjacent shelf from Luo et al. (2012) and 106 samples of YZE core from Chen et al. (2014).

Eight Sea charts from 1864 to 2013 were also collected to help understand the geomorphological change of the Yangtze estuary through the Digital Elevation Model (DEM). Among them, the sea charts at the years of 1864, 1879, 1932, 1958, 1979 are 1:100, 000, and those of 1993, 2002, and 2013 are 1:50, 000. The sea charts at the years of 1864 and 1879 were surveyed during 1842–1961 and 1879–1880 respectively by British Admiralty. The others were all surveyed by related navy department of China, in which the years of 1979, 1993, 2002 and 2013 were surveyed during 1976–1978, 1990–1993, 2000–2001 and 2010–2013 respectively and the years of 1926 and 1958 were the surveys of their own year. The water depth data derived from all the sea charts were corrected based on the unified theoretical depth benchmark in the Yangtze estuary.

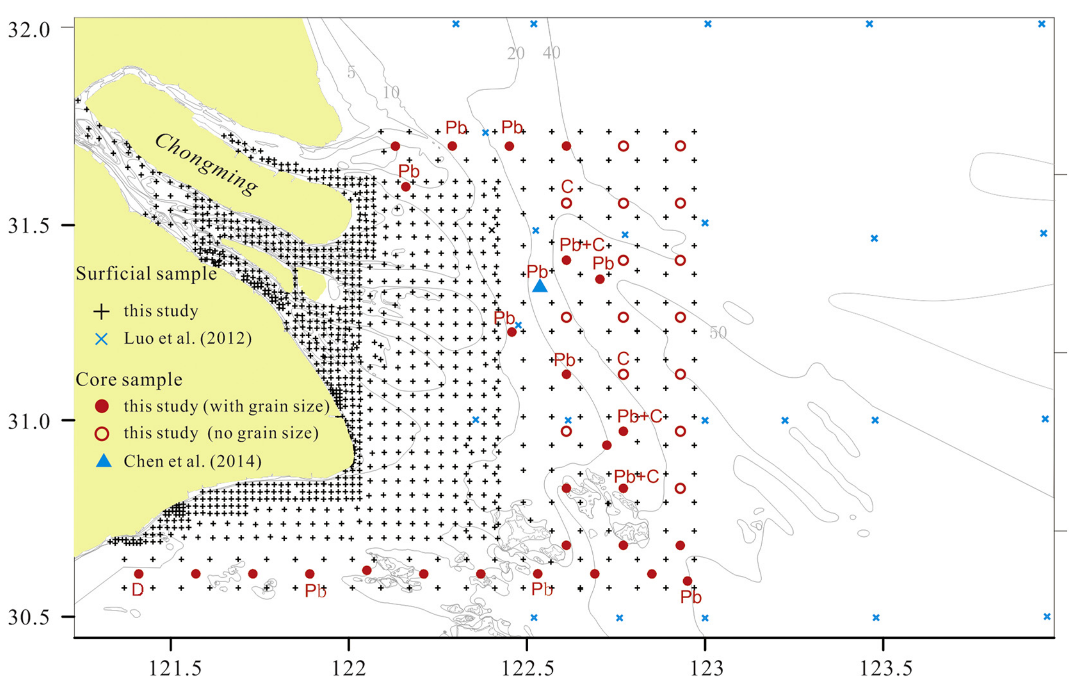

Fig. 1. Location of surficial sediment samples and cores in the Yangtze subaqueous delta. Labels of Pb or C next to the core represent the cores dated by ^{210}Pb and ^{137}Cs or AMS ^{14}C respectively.

Table 1
Core location and sampling for analysis in the Yangtze subaqueous delta.

Core ID	Latitude N	Latitude E	Core depth (m)	Water depth (m)	^{210}Pb and ^{137}Cs	Grain size	AMS ^{14}C	Source
CDZS1	31.69	122.08	3.4	−6.19		50		This study
CDZS2	31.69	122.25	3.4	−16.75	100	178	2	
CDZS3	31.69	122.42	2.1	−23.92	52	78		
CDZS4	31.69	122.59	2.5	−34.6		23		
CDZS5	31.69	122.76	1.7	−36.8		7		
CDZS6	31.69	122.93	1.9	−37.4		7		
CDZS7	31.55	122.59	1.5	−29.7		15	1	
CDZS8	31.55	122.76	2.75	−32.8		10		
CDZS9	31.55	122.93	2	−35		7		
CDZS10	31.40	122.59	3	−36.8	67	49	2	
CDZS11	31.41	122.76	3	−45.5		9		
CDZS12	31.41	122.93	1.65	−35.4		6		
CDZS13	31.26	122.59	3.1	−29.5		9		
CDZS14	31.26	122.76	3.15	−46.4		9		
CDZS15	31.26	122.93	2.25	−65.5		8	1	
CDZS16	31.12	122.59	3.35	−20.7	72	54	1	
CDZS17	31.12	122.76	3.25	−35.7		9	1	
CDZS18	31.12	122.93	3	−57		11		
CDZS19	30.97	122.59	3.35	−19.5		12		
CDZS20	30.97	122.76	3	−25	66	50	2	
CDZS21	30.97	122.93	3.1	−42		11		
CDZS22	30.83	122.59	3.1	−9		32		
CDZS23	30.83	122.76	3.05	−27.5	68	51	4	
CDZS24	30.83	122.93	3.15	−39.5		11		
CDZS25	30.68	122.59	3.05	−17.6		31		
CDZS26	30.68	122.76	3.1	−56		32		
CDZS27	30.68	122.93	3.1	−42		32		
CDZS28	30.60	121.34	3.3	−9.9	100	170		
CDZS29	30.60	121.51	3.15	−9		32		
CDZS30	30.61	121.68	3.1	−8.1		31		
CDZS31	30.61	121.84	3.2	−8.6	100	160		
CDZS32	30.62	122.01	3.05	−8.47		31		
CDZS33	30.61	122.18	3.12	−10.4		32		
CDZS34	30.61	122.34	1.7	−14.8		18		
CDZS35	30.61	122.51	3.15	−22.5	100	165	2	
CDZS36	30.61	122.68	3.3	−29		34		
CDZS37	30.61	122.84	3.1	−35		32		
CDZS38	30.94	122.71	3.4	−19.9	100	170		
CDZS39	31.36	122.69	3.1	−47	100	155	2	
CDZS40	30.59	122.95	3.05	−49	100	152	1	
QHCS1	31.59	122.12	4	−5.50	30	45		
QHYS2	31.22	122.43	4	−10.50	20	78		
YZE	31.33	122.50	2.3	−26.40	48	106		Chen et al. (2014)

3. Results

3.1. Spatial distribution of grain size in the surficial sediments of the Yangtze subaqueous delta

The median grain size (D50) of the Yangtze subaqueous delta shows a general trend of coarse-fine-coarse from the estuary to the shelf (Fig. 2).

In terms of silt content (30% and 60%), it can be divided into four depositional zones (I–IV; Fig. 2). Coarse particles (silt of < 30% and sand of > 60%) are deposited near the river mouth, forming the estuarine sand bar (Zone I; Fig. 2). Finer particles (silt of > 60%) are trapped offshore, forming the muddy prodelta (Zone II; Fig. 2). Both zones are characteristic of a unimodal distribution on the grain size frequency curve (coarse peak of Zone I and fine peak of Zone II; Fig. 2). Toward the shelf, the sediment becomes coarse again, forming a delta-shelf transitional zone with silt of 30–60% (Zone III; Fig. 2). The mode of the grain size frequency curve changes to a typically bimodal distribution (Zone III; Fig. 2). The shelf area is mainly occupied by sand (sand of > 60%) with a coarse unimodal distribution on the frequency curve (Zone IV; Fig. 2).

3.2. Sediment grain size of the Yangtze subaqueous cores

The grain size of 11 typical cores is shown in Fig. 3, spatially covering each depositional zone of the Yangtze subaqueous delta (I–IV; Fig. 2).

3.2.1. Sediment grain size of the cores in Zone I

Core CDZS1 is located in the north part of Zone I and is a typical core of the estuarine sand bar in the Yangtze subaqueous delta (Fig. 2). The core can be divided into two layers at a core depth of 2.3 m in terms of grain size parameters (Fig. 3). The upper layer (0–2.3 m) is much coarser than the lower layer (2.3–3.3 m), having a median grain size (D50) of 36.7–155.2 μm and 11.3–66.6 μm, respectively (Fig. 3). Sand dominates the upper layer, accounting for 31.4–91.6%, while silt (43.4–75%) is the main component in the lower layer (Fig. 3).

3.2.2. Sediment grain size of the cores in Zone II

CDZS2, CDZS20, and CDZS38 are located in Zone II, in which CDZS2 is in the north part and the others in the south part, the depocenter of the subaqueous delta also called "mud region" (Fig. 2).

The cores of this zone are generally fine with a D50 range of 4.5–85 μm and silt content reaches 50–80% (Fig. 3). Especially the two cores of the depocenter (CDZS20 and CDZS38) are much finer and have little change on grain size throughout the core (Fig. 3). By contrast, the

Table 2
AMS ^{14}C ages of core samples in the Yangtze subaqueous delta.

Core	Depth (m)	Material	Meterial^{14}C age(a BP)	Conventional age(a BP)	Calibrated age 1 sigma (cal yr BP)	Probability	Calibrated age 2 sigma (cal yr BP)	Probability	Laboratory No.
CDZS7	0.45	Shell fragment	6190 ± 40	6620 ± 40	6990 ± 85	1	6995 ± 155	1	349,896
CDZS10	0.35	Shell fragment	980 ± 30	1390 ± 30	805 ± 65	1	800 ± 110	1	349,897
CDZS10	2.78	Shell fragment	580 ± 30	1000 ± 30	490 ± 40	1	500 ± 100	1	349,898
CDZS17	0.95	Shell fragment	230 ± 30	620 ± 30	75 ± 70	0.97	120 ± 115	1	349,900
CDZS20	1.88	Shell fragment	290 ± 30	660 ± 30	170 ± 75	1	150 ± 110	0.93	349,903
CDZS23	1.66	Shell fragment	200 ± 30	610 ± 30	70 ± 70	1	115 ± 115	1	349,905

core of the north delta (CDZS2) has a coarsening trend on the top layer (0–0.5 m), with increasing sand content to 30–70% (Fig. 3).

3.2.3. Sediment grain size of the cores in Zone III

CDZS3, YZE, CDZS39, CDZS10, CDZS27, and CDZS40 are all located in Zone III, in which CDZS3, YZE, CDZS39, and CDZS10 are in the north subaqueous delta and the others are in the south part (Fig. 2). All the cores of this zone have significant changes on grain size throughout the core.

Among the cores of the north subaqueous delta, YZE, CDZS39, and CDZS10 have similar changes throughout the core on grain size (Fig. 3). All these cores show a trend of coarsening on the top layer (0–1 m in YZE; 0–0.7 m in CDZS39; 0–0.7 m in CDZS10), with significantly increasing sand content (Fig. 3). Although silt (20–80%) is dominant in the three cores, CDZS10 is relatively coarser than the other two cores. While, CDZS3 has a coarse-fine-coarse trend upwards in the core. The upper layer (0–1 m) is much finer than the lower layer (1–2.1 m) and silt and sand are the dominant components of the two layers respectively (Fig. 3). Of note, the top 0.3 m of the core seems to be coarsening in the upper layer (Fig. 3).

The cores of the south part (CDZS27 and CDZS40) have similar trends of fining upwards in the core (Fig. 3). The upper cores (0–1.7 m in CDZS27; 0–1.9 m in CDZS40) are mainly composed of silt (50–80%), while sand can reach to ~60% in the lower cores. Of note, coarsening occurs on the top 0.2 m of CDZS40 with sand increasing to 30%. However, such a record is missing in CDZS27 due to low sampling resolution on grain size (Fig. 3).

3.2.4. Sediment grain size of the cores in Zone IV

CDZS4 in the north delta is a typical core of Zone IV (Fig. 2). The core is mainly composed of sand (57.5–95.3%). The grain size changes little throughout the core, with a narrow Md range of 121–176 μm (Fig. 3).

3.3. Chronology based on ^{210}Pb, ^{137}Cs and AMS^{14}C of the Yangtze subaqueous cores

Although ^{210}Pb and ^{137}Cs of 15 cores were tested in the Yangtze subaqueous delta, the results of most cores were not ideal. This may be related to the complex sedimentary environment of large river estuary, receiving ^{210}Pb and ^{137}Cs not only from the atmosphere but also from the river and sea (Wei et al., 2007; Zhang et al., 2008a; Xie et al., 2012).^{210}Pb and ^{137}Cs results of three cores are shown here to help determine the approximate sedimentation rate in this region (Fig. 4).

$^{210}Pb_{ex}$ activities are all below 300 Bq kg^{-1} in the three cores and generally decrease exponentially with the core depth ($R^2 > 0.6$). Based on the CIC model, the average sedimentation rates of the three cores can be estimated as 3.28, 3.69, and 2.63 cm/yr, respectively (Fig. 4). Of note, sediment mixing occurs on the top of the three cores (Fig. 4).

^{137}Cs activities are generally lower than 8 Bq kg^{-1} in YZE, CDZS10 and CDZS2 (Fig. 4). The first detectable ^{137}Cs activity occurs at the core depth of 104 cm, 224 cm, and 202 cm in the three core respectively, indicating the first atmospheric deposition of radionuclide in 1950s (Huh and Su, 1999). The corresponding sedimentation rates of the upper layer since the 1950s are 1.85, 3.73, and 3.37 cm/yr in the three cores, respectively (Fig. 4). Comparing the sedimentation rates derived from $^{210}Pb_{ex}$, it is significantly lower in core YZE and slightly higher in core CDZS20 (Fig. 4).

The AMS ^{14}C ages of the cores are older comparing to those derived from ^{210}Pb and ^{137}Cs in CDZS10, possibly because shell fragments used for measurement might be transported from the shelf (Fig. 4; Table 2). The ages of CDZS17, CDZS20 and CDZS23 are not much different from those of ^{210}Pb and ^{137}Cs, if considering the age error by AMS ^{14}C. Hence, these cores prefer chronology of ^{210}Pb and ^{137}Cs in this study. The age of 6995 cal. yr BP. at 0.45 m of CDZS7 suggests no modern deposition in the shelf area (Table 2).

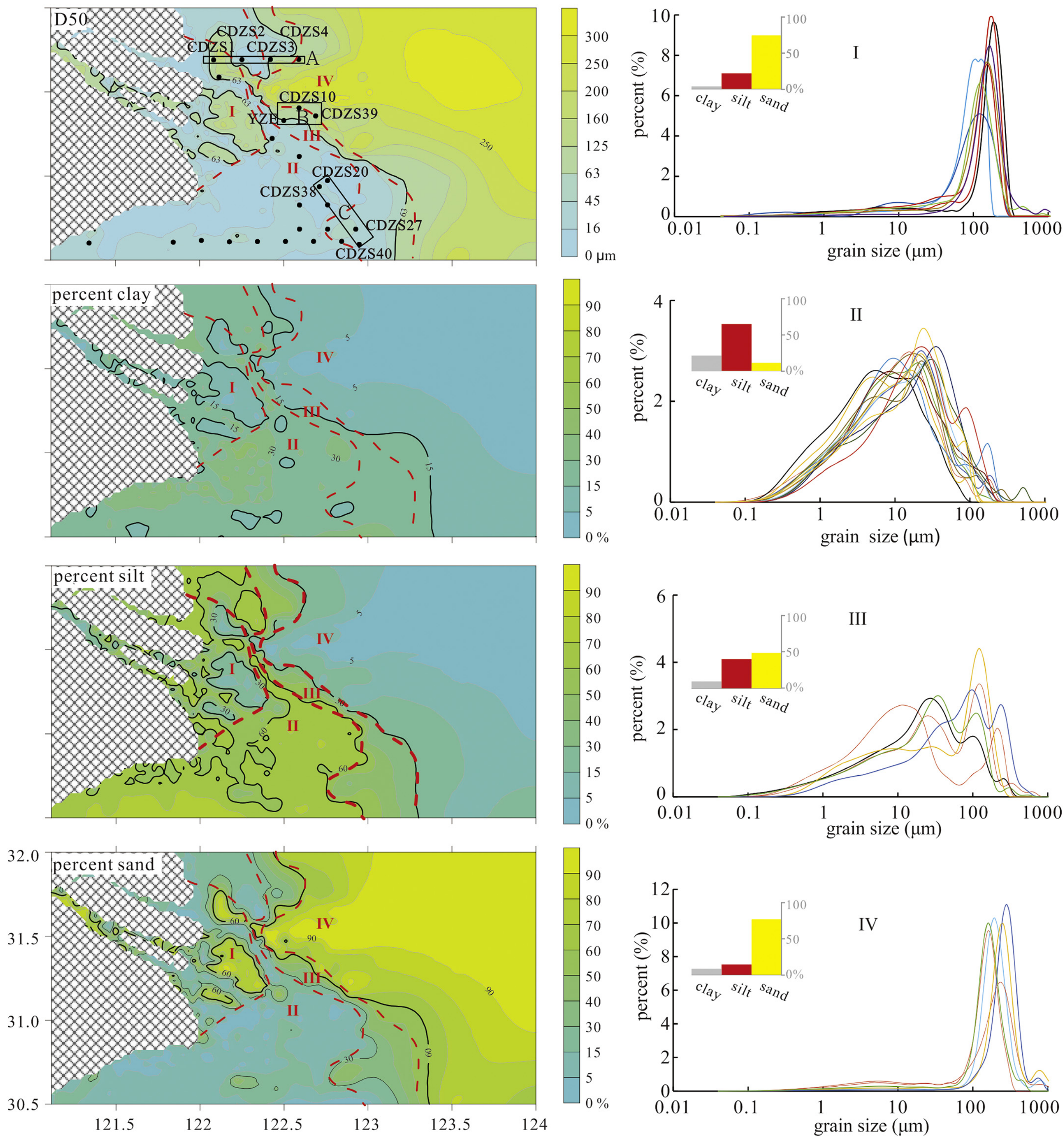

Fig. 2. Sediment composition in the surficial sediments of the Yangtze subaqueous delta. The left column shows median grain size (D50), percent clay, percent silt and percent sand downwards. The right column shows the frequency curves of grain size for each of the respective depositional zones. I, II, III and IV denote sedimentary zones according to the silt percent. I-estuarine sand bar, II-prodelta, III-delta-shelf transition zone, IV-residual sand.

3.4. Geomorphological change of the Yangtze estuary in the past 150 years

The DEMs based on sea charts show the progradation of the delta plain and southward migration of the main channel of the Yangtze estuary from 1864 to 2013 (Fig. 5). The North Branch was silted rapidly during the period of 1864–1958, manifested by merging estuarine sand bars northward to the shore (A-D; Fig. 5). Meanwhile, a series of estuarine sand bars began to form in the South Branch, such as Changxing, Hengsha, and Jiuduansha islands (A-D; Fig. 5). Since 1958, the upper reach of the North Branch has been severely blocked and the sand bars and tidal flats of the South Branch began to accumulate (E-H; Fig. 5).

The area and capacity of branch channels also indicates shrinking of the North Branch quantitatively (I and J; Fig. 5). Over the past 150 years, the South Branch has decreased by 20% and 10% in the channel area and capacity, of which the capacity has changed very little

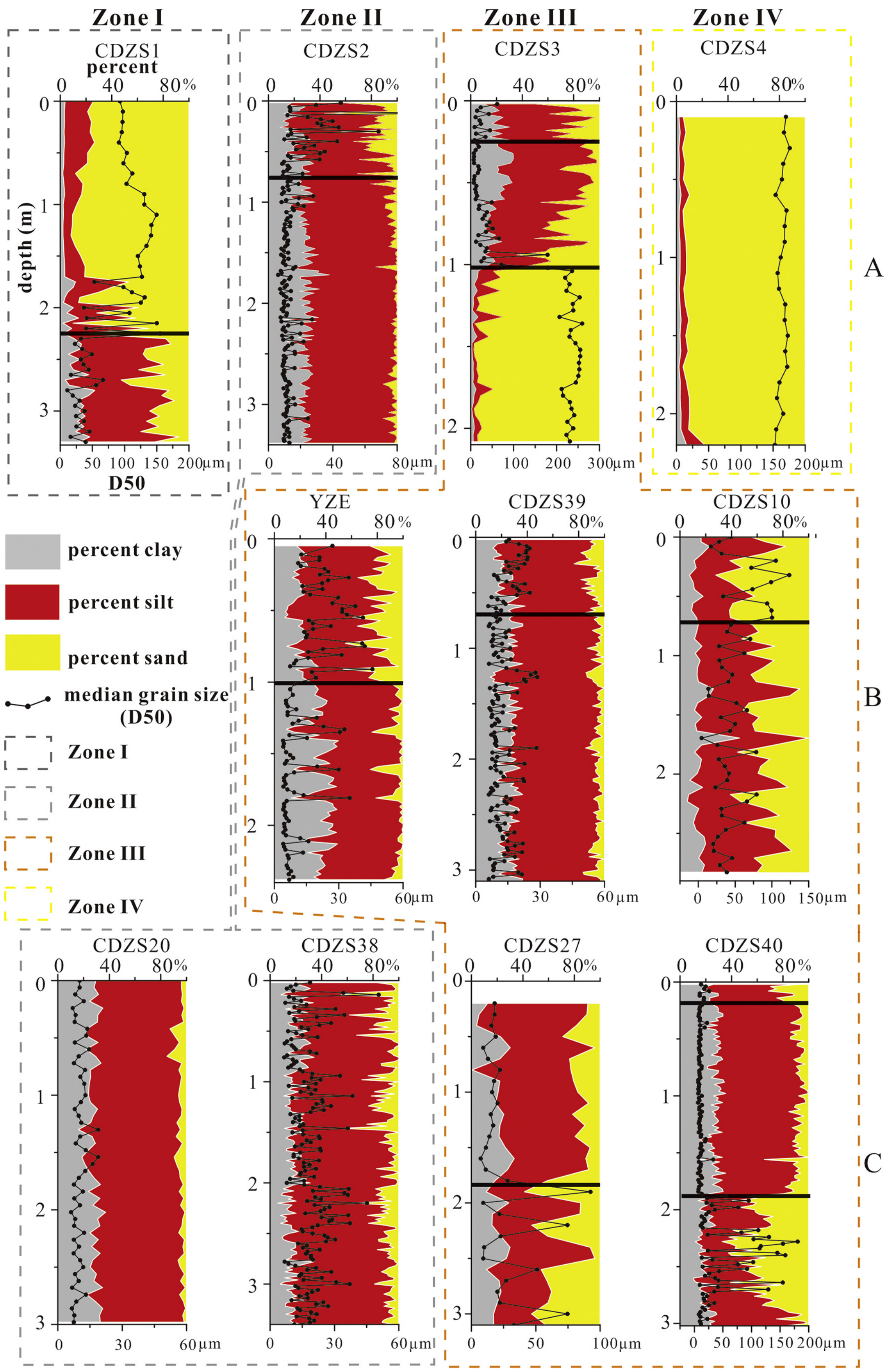

Fig. 3. Grain size of the typical cores in the Yangtze subaqueous delta. The core locations are marked in the profiles of A-C in Fig. 2. The black horizontal line in the core shows the depth of grain size change.

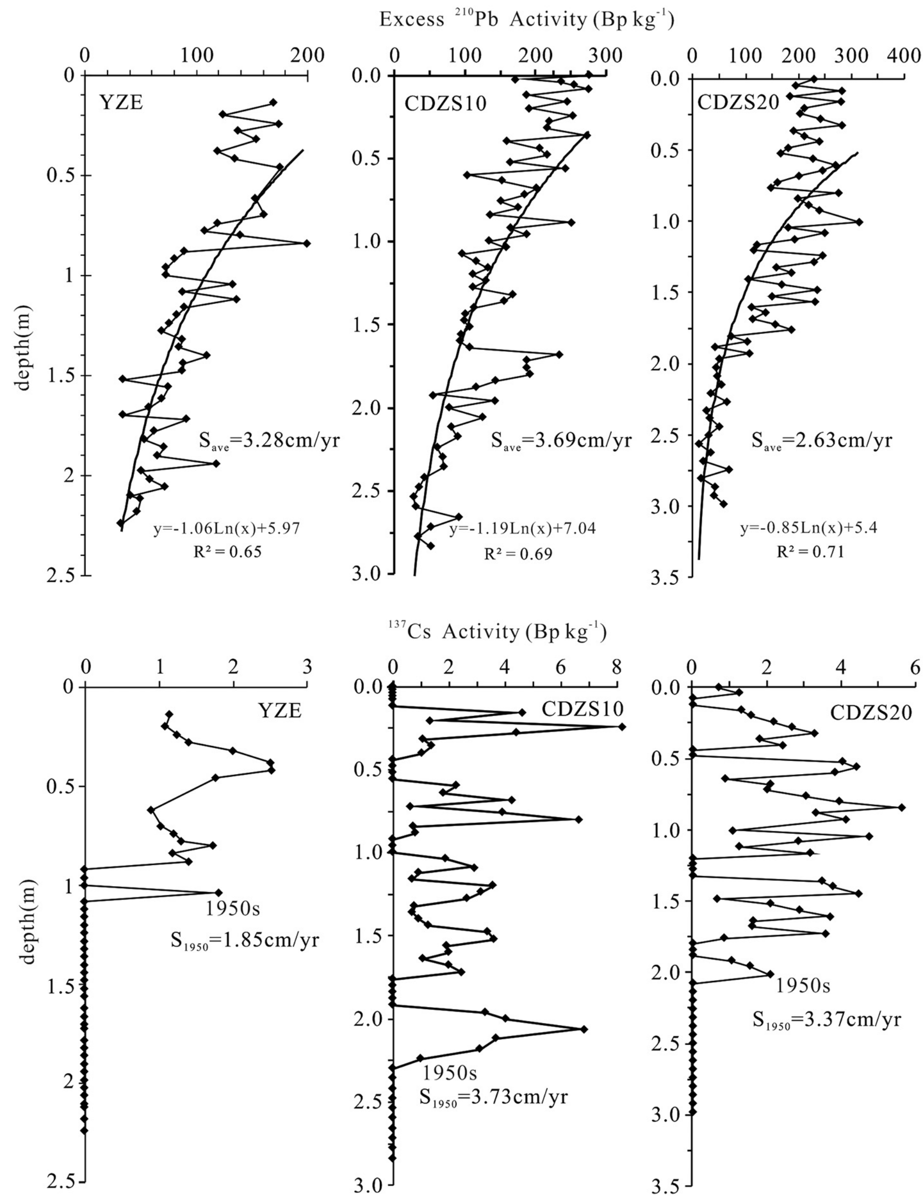

Fig. 4. $^{210}Pb_{ex}$ and ^{137}Cs activities of the Yangtze subaqueous cores. Core YZE is from Chen et al. (2014). CDZS10 and CDZS23 are referred to Zhan et al. (2016). S_{ave} derived from ^{210}Pb means the average sedimentation rate of the whole core and S_{1950} from ^{137}Cs means the sedimentation rate of the upper core since 1950s.

since 1879. Comparatively, the area and capacity of the North Branch have dropped by 70% and 80%, most of which occurred during the period of 1864–1958. Since 1958, the capacity of North Branch has been generally below 25% of the South Branch, indicating a weak capacity for water and sediment to pass through.

4. Discussion

4.1. Surficial sedimentary regime in the Yangtze subaqueous delta

Yangtze-derived sediment into the estuary is mainly composed of silt, thus silt percentage is used for sedimentary zone identification in this study (Fig. 2; Yang et al., 2003). When the river meets the sea, the fluvial sediments deposit fining seawards in the estuary due to marine force jacking. This fining trend is seen from Zone I of the estuarine sand bar to Zone II of the prodelta (Fig. 2). Unimodal distribution on the grain size frequency curve in the two zones implies a fluvial-dominated deposition (Fig. 2). However, the sediment then becomes coarse toward the continental shelf from Zone III to Zone IV (Fig. 2). The frequency curve of the coarse unimodal in Zone IV implies the total control of marine force. The deposits here are also called "residual sand", which was formed during the low sea-level period pre-Holocene and reformed by marine force thereafter (Emery, 1968; Shen, 1985). Zone III, located between the estuary and shelf, is under the dual influences of fluvial and marine force shown by the bimodal frequency curve of grain size (Fig. 2).

It can be seen that the sediment is fining and then coarsening from the estuary to the shelf, revealing the weakened influence of fluvial force and strengthened influence of marine force (Qin et al., 1987; Luo et al., 2012). The delta-shelf transition zone (Zone III) is the boundary affected by fluvial force and it is very sensitive once the hydrodynamic balance is broken between fluvial and marine force.

4.2. Grain size proxy sensitive to hydrodynamic change in the Yangtze subaqueous delta

Sediment grain size is closely related to hydraulic sorting as well as sediment source, especially in the river estuary. In other words, the

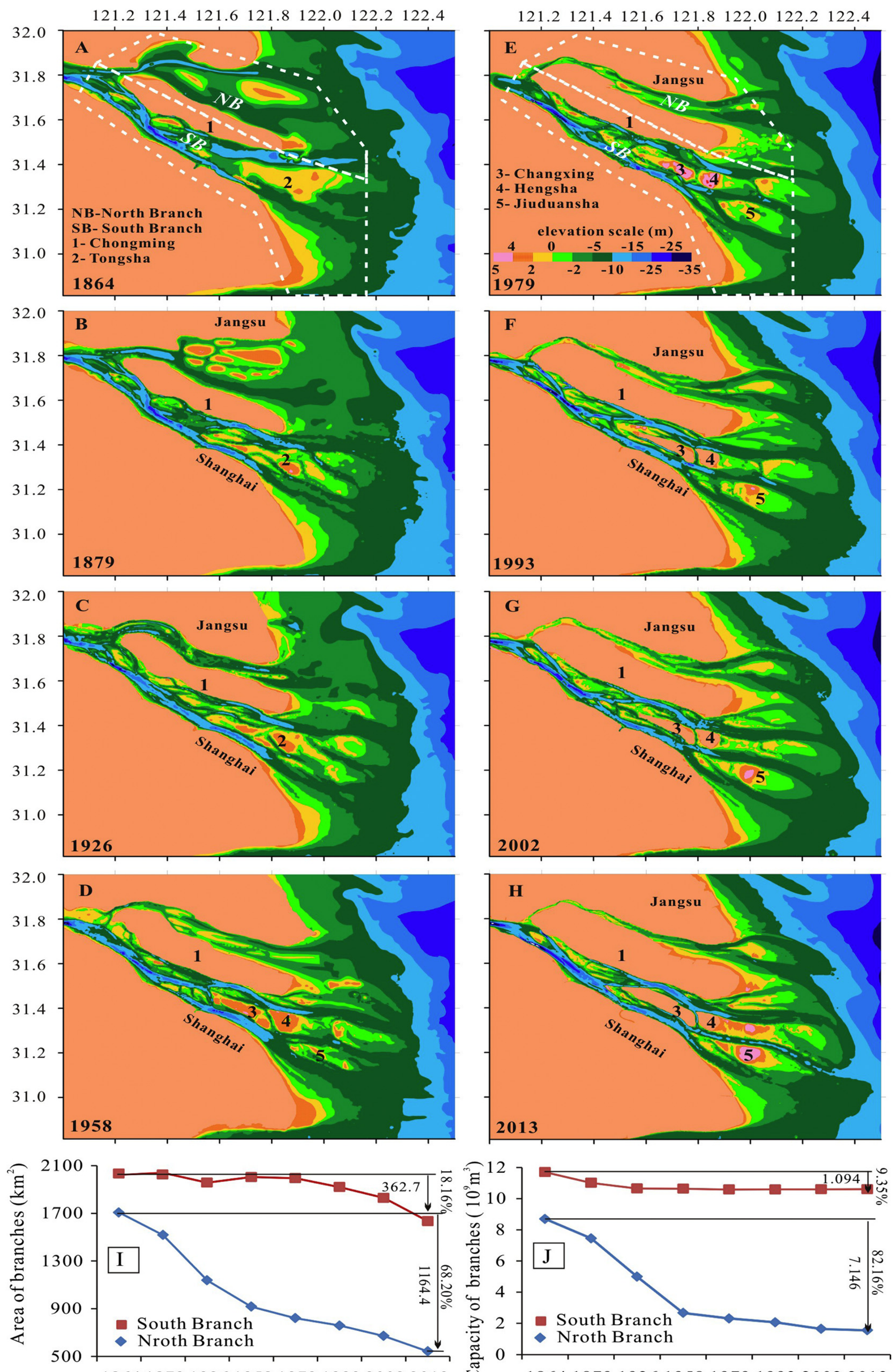

Fig. 5. DEMs of the Yangtze estuary based on sea charts from 1864 to 2013 (A-H) and channel area (I) and capacity (J) of the South Branch and the North Branch.

grain size of the bulk sediment is a comprehensive result overlaid by various factors. Comparatively, a certain fraction of grain size extracted using a "standard deviation vs. grain size" method is more sensitive to the change of some environmental factors (Sun et al., 2003; Xiao et al., 2006).

This study extracts two fractions of 16–63 μm (Fraction 1) and > 63 μm (Fraction 2) which are the most sensitive components in the typical cores of the Yangtze subaqueous delta (Fig. 6a). Fraction 1 is

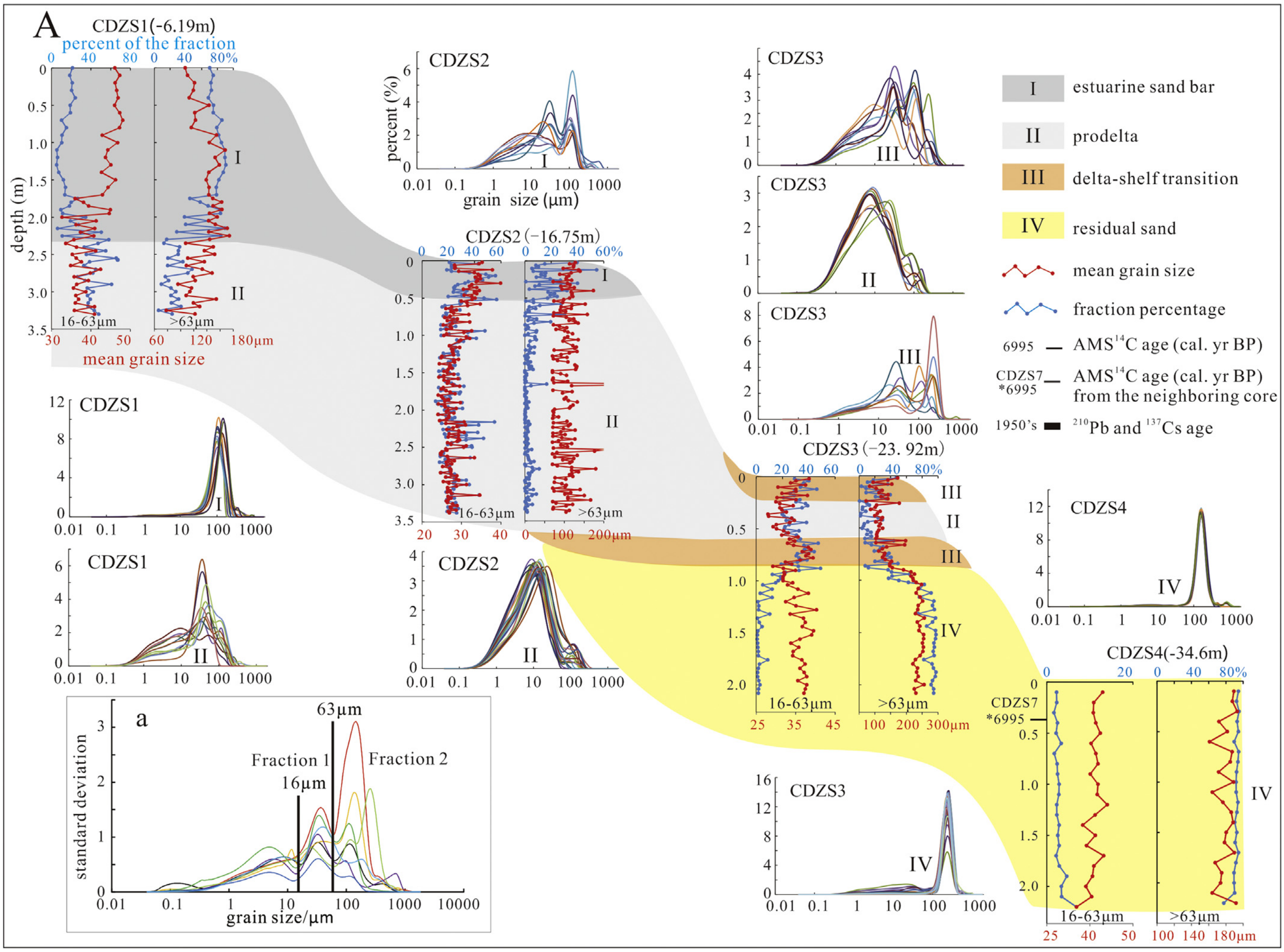

Fig. 6. Percentage and mean grain size (Mz) of the sensitive fractions and typical frequency curves in the Yangtze subaqueous cores. Sensitive fraction determination of typical cores refers to the inset figure a. Profiles of A-C see Fig. 2. Sedimentary zones of I-IV in the cores are identified based on the analogue of grain size parameters with the surficial sediment in Fig. 2. Sediment flux and runoff of the Yangtze River during 1955–2017 are shown in the inset figure b and sourced from the Changjiang Water Resources Commission and the Data-sharing Network of China Hydrology (http://www.hydrodata.gov.cn).

the main component of the prodelta and delta-shelf transition zones (Zone II and III, Fig. 2) and its variation in the core reflects the change of balance between fluvial and marine force in the subaqueous delta (Zhang et al., 2008b; Fan et al., 2011). Fraction 2 is the major component of estuarine sand bar and residual sand (Zone I and IV, Fig. 2) and its variation in the core should be interpreted as the control of fluvial or marine force depending on the core location (Fig. 2; Zhang et al., 2007). The percentages of the two fractions are sometimes complementary to each other upwards in the cores, because they are relative when calculating (such as CDZS1, CDZS3; Fig. 6A). Comparatively, the mean grain size (Mz) of the two fraction is completely unrelated and its variation in the core can better help determine which fraction is the active factor in the change.

4.3. Sedimentary progradation of the subaqueous delta in the past few hundred years

In the past few hundred years, the main channel of the Yangtze estuary has moved southward and the deposition center occurred in the south subaqueous delta (Fig. 5; Wei et al., 2007; Wang et al., 2013). Limited to the core length of this study, the delta progradation process should be revealed more easily in the north region, which is well recorded by the grain size proxy of profiles CDZS1–4 outside the North Branch (Fig. 6A).

The mean grain size (Mz) of Fraction 2 (> 63 μm) changes positively with its percentage throughout core CDZS1, indicating that this fraction controls the change of grain size in the core and can be regarded as a hydrodynamic proxy (Fig. 6A). Coarsening dramatically above the core depth of 2.5 m on Mz of Fraction 2 possibly reflects the controlling of fluvial force here, considering the core location. In addition, the grain size frequency curve also changes from fine unimodal to coarse unimodal upwards in the core correspondingly, which are similar to prodelta (Zone II) and estuarine sand bar (Zone I) in the surficial sedimentary regime, respectively (Figs. 2 and 6A). All these features indicate that sedimentary environment in the region of CDZS1 changes from prodelta to estuarine sand bar. Similarly, coarsening on the top of CDZS2 reflected by Mz of Fraction 1 indicates enhanced fluvial force and here is experiencing a transition from prodelta to estuarine sand bar (Fig. 6A). It is speculated that the time for such an environment change may begin since 1800–1900, according to the sedimentation rates derived from nearby cores (~1 cm/yr, Wang et al., 2013) and rapid accumulation seaward of the North Branch during 1864–1958 (Fig. 5). Meantime, sedimentary environment changes from residual sand (Zone IV) and delta-shelf transition zone (Zone III) to prodelta (Zone II) successively at the location of core CDZS3(Fig. 6A). This is supported by the frequency curves from coarse unimodal,

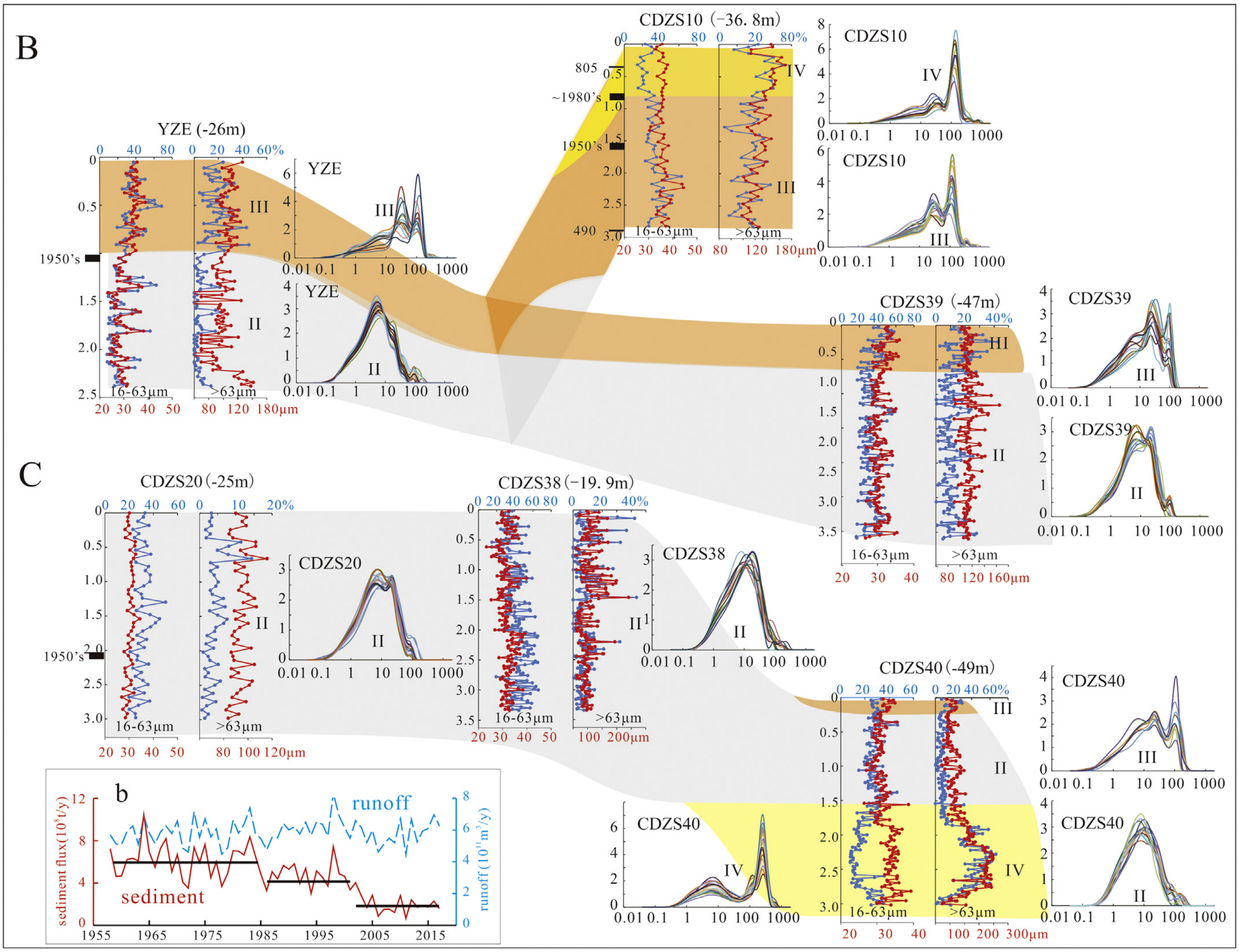

Fig. 6. (*continued*)

bimodal to fine unimodal upwards in the core, resembling those of Zone IV, Zone III, and II in the surficial sediments, respectively (Figs. 2, 6A). In addition, fining Mz of Fraction 1 upwards in the core also indicates weakening marine force here(Fig. 6A). During the same period, the location of CDZS4 are still occupied by residual sand (Zone IV; Fig. 6A). Overall, the profile of CDZS1–4 reveals that the north subaqueous delta has prograded rapidly to the sea during the past few hundred years, and the prodelta has once expanded to the location of CDZS3 where it currently belongs to the delta-shelf transition zone (Figs. 2, 6A). This may be benefited from the relatively large amounts of water and sediment flowing through the North Branch into the sea before the 1950s (Fig. 5; Shen, 2001; Shen et al., 2003).

In addition, a similar process of progradation is also recorded by CDZS40 in the south subaqueous delta, with a sedimentary change from residual sand to prodelta upwards in the core (Fig. 6C). Although the timing of this change cannot be determined, it certainly corresponds to the increasing water and sediment flux through the South Branch since 1800–1900 (Shen, 2001; Shen et al., 2003; Fig. 5).

4.4. Sedimentary transition of the Yangtze subaqueous delta since 1950s

The cores in the delta-shelf transition zone (Zone III) show a coarsening trend on grain size within the top 1 m generally (Figs. 3 and 6). In which, Fraction 1 (16–63 μm) is the sensitive grain size to hydrodynamic change in the cores of CDZS3, YZE, CDZS39, and CDZS40 (Fig. 6A, B and C). The increasing Mz of Fraction 1 on the top of these cores is indicative of relatively enhancing marine force. Meantime, the bimodal frequency curves resembling Zone III dominate the top of the cores, which are different from the unimodal frequency curves below. All these features suggest that the region has changed from prodelta (Zone II) to delta-shelf transition zone (Zone III, Figs. 2, 6). For core CDZS10 located near the zone of residual sand, the sensitive grain size is Fraction 2 (> 63 μm). The increasing Mz on the top 0.7 m of the core indicates controlling of marine force, which is also support by the old shell possibly transported from the shelf (dating to 805 cal. yr BP. at the core depth of 0.4 m, Table 2; Fig. 6B). It seems that the sedimentary environment has been changed from delta-shelf transition zone to residual sand in terms of the frequency curves (Fig. 6B).

The sedimentary changes on the abovementioned cores reveal that a sedimentary transition (from progradation to retrogradation) of the Yangtze subaqueous delta has initialled in the delta-shelf transition zone (Zone III), especially in the north delta (e.g. profiles A and B, Fig. 6). The timing of the transition is hard to determine precisely in each core due to the chronology constrained by complex sedimentary environment here. Despite this, one thing is certain that the sedimentary transition does not occur simultaneously for all of the cores. Constrained by ^{210}Pb and ^{137}Cs of YZE and CDZS10, the sedimentary transition likely occurred in 1950s and 1980s respectively (Figs. 4 and 6B). In the case of CDZS40, located in the south subaqueous delta, sedimentary transition may happen more recently due to coarsening only on the top 20 cm of the core. The nearby core from Luo et al. (2012) also showed such a coarsening trend on the top core.

4.5. Sedimentary transition in the north subaqueous delta: an inspiration for the response of the Yangtze delta to the future decline of sediment supply

We speculate that the sedimentary transition since 1950s in the abovementioned cores in the north of Zone III is possibly related to spatial diversion change of water and sediment in the estuary and sediment decline from the Yangtze River.

Hankou station located in the middle mainstream recorded the Yangtze River flow since 1865 and the sediment flux was reconstructed accordingly (Wang et al., 2008). No significant change in water and sediment flux is found around 1950s, therefore the fluvial change is not the reason for the relatively enhancing marine force and recent sedimentary transition in the north subaqueous delta (Fig. 6). Adjustment of water and sediment diversion in the estuarine branches in the past few hundred years may be the primary reason. The North and South Branches are the first-level branch of the Yangtze estuary (Fig. 5). Until the beginning of the 20th century, the North Branch was the main channel for the Yangtze sediments flowing into the sea (Shen, 2001; Shen et al., 2003). Subsequently, the main channel shifted to the South Branch, but the North Branch still discharged 25% of the Yangtze flow (Shen, 2001; Shen et al., 2003). By 1950s, the North Branch was shrinking sharply and discharging less than 5% of the flow, caused by the severe flood of 1954 and human reclamation in 1958 (Shen, 2001; Yun, 2010). The DEMs based on sea charts also show that the tidal flats around the North Branch have hardly increased since 1950s, replaced by the rapid expansion of those flats near the South Branch (Fig. 5). The marine power was relatively enhancing in the delta-shelf transition zone with the shrinking of the North Branch since 1950s, which caused sediment coarsening in the north subaqueous delta by re-suspending and transporting fine sediments out (Fig. 6A and B; Shen et al., 1986; Li et al., 1994). Such a sediment diversion adjustment of estuarine branches has led to retrogradation of the north subaqueous delta and the southward migration of the subaqueous depocenter, reflected by the retreating north prodelta that once expanded to the modern delta-shelf transition zone (Zone III, Figs. 2, 6A and B).

The Yangtze sediment flux has decreased significantly since 1980s, causing the retrogradation further intensified that the delta-shelf transition zone has begun to transform into residual sand zone in the north subaqueous delta (CDZS10, Fig. 6b and B; Wang et al., 2008; Yang et al., 2011).

It is worth noting that the surficial coarsening in the south delta-shelf transition zone is probably related to drastic sediment decline since the impoundment of the Three Gorges Dam in 2003 (CDZS40, Fig. 6b and C). This means that the Yangtze subaqueous delta has been experiencing a full sedimentary transition. However, retrogradation has not been observed in the cores of the modern depocenter (south prodelta), indicating that the riverine sediment decline has not caused sedimentary transition in this region by far.

In summary, the delta-shelf transition zone is the most sensitive to sediment supply adjustment from the river basin and estuarine channels and it is the initial place where sedimentary transition happens once sediment supply declines. Sedimentary transition of the north subaqueous since 1950s can provide an insightful reference for the sedimentary response of the Yangtze delta to further decline of sediment supplyin the future.

5. Conclusions

From the estuary to the continental shelf, a sedimentary system of estuarine sand bar, prodelta, delta-shelf transition zone, and residual sand is distributed in the Yangtze subaqueous delta, manifested by first fining and then coarsening seawards on the surficial sediments under the balance of fluvial and marine force. In the past few hundred years, the subaqueous delta has been generally prograded seaward following this sedimentary system spatially, manifested by generally fining upwards in the cores of the main subaqueous delta. However, sediment coarsening occurs on the top of the cores in the delta-shelf transition zone, implying a recent retrogradation process. Constrained by the results of ^{210}Pb and ^{137}Cs, the sedimentary transition from progradation to retrogradation occurred since 1950s and was intensified after 1980s in the north part of the delta-shelf transition zone, mainly caused by channel shrinking of the North Branch and riverine sediment decline. Comparatively, such a sedimentary transition is not significant in the south part of the delta-shelf transition zone. But it is worth noting that surficial coarsening in the core (of the south part of Zone III) is probably related to drastic sediment decline since 2003 when the Three-Gorges Dam closed, which means that the Yangtze subaqueous delta has probably been in a full sedimentary transition. The sedimentary transition of the north subaqueous delta can provide an insightful reference for the sedimentary response of the Yangtze delta to further decline of sediment supply in the future.

Declaration of Competing Interest

The authors declare no conflict of interest to disclose.

Acknowledgements

This research was funded by the National Natural Science Foundation of China (grant Nos. 41706098, 2016YFE0133700, 41671007, 41620104004, 41771226), and the Fundamental Research Funds for the Central Universities. The authors are debt in the reviewers' valuable comments.

References

Besset, M., Anthony, E.J., Bouchette, F., 2019. Multi-decadal variations in delta shorelines and their relationship to river sediment supply: an assessment and review. Earth-Sci. Rev. 193, 199–219.
Blum, M.D., Roberts, H.H., 2009. Drowning of the Mississippi Delta due to insufficient sediment supply and global sea-level rise. Nat. Geosci. 2, 488–491.
Carozza, J.M., Micu, C., Mihail, F., Carozza, L., 2012. Landscape change and archaeological settlements in the lower Danube valley and delta from early Neolithic to Chalcolithic time: a review. Quat. Int. 261, 21–31.
Chen, Z.Y., Song, B.P., Wang, Z.H., Cai, Y.L., 2000. Late Quaternary evolution of the subaqueous Yangtze Delta, China: sedimentation, stratigraphy, palynology, and deformation. Mar. Geol. 162 (2–4), 423–441.
Chen, Z.Y., Wang, Z.H., Schneiderman, J., Tao, J., Cai, Y.L., 2005. Holocene climate fluctuations in the Yangtze delta of eastern China and the Neolithic response. The Holocene 15 (6), 915–924.
Chen, J., Zhao, B., Zhan, Q., 2014. Grain size of recent sediments in the north of Changjiang Subaqueous delta and its implication of estuarine hydrodynamics. Acta Sedimentol. Sin. 32 (4), 692–699 (in Chinese with English abstract).
Chu, Z.X., Sun, X.G., Zhai, S.K., Xu, K.H., 2006. Changing pattern of accretion/erosion of the modern Yellow River (Huanghe) subaerial delta,China: Based on remote sensing images. Mar. Geol. 227 (1/2), 13–30.
Dai, Z.J., Liu, J.T., Wei, W., Chen, J.Y., 2014. Detection of the Three Gorges Dam influence on the Changjiang (Yangtze River) submerged delta. Sci. Rep. 4, 6600.
Dai, Z.J., Fagherazzi, S., Mei, X., Chen, J., Meng, Y., 2016. Linking the infilling of the north Branch in the Changjiang (Yangtze) estuary to anthropogenic activities from 1958 to 2013. Mar. Geol. 379, 1–12.
Emery, K.O., 1968. Relict sediments on continental shelves of world. AAPG Bull. 52 (3), 445–464.
Fan, D.J., Qi, H.Y., Sun, X.X., Liu, Y., Yang, Z.S., 2011. Annual lamination and its sedimentary implications in the Yangtze River delta inferred from High-resolution biogenic silica and sensitive grain-size records. Cont. Shelf Res. 31, 129–137.
Giosan, L., Syvitski, J., Constantinescu, S., Day, J., 2014. Protect the world's deltas. Nature 516, 31–33.
Huh, C.A., Su, C.C., 1999. Sedimentation dynamics in the East China Sea elucidated from ^{210}Pb, ^{137}Cs and $^{239,240}Pu$. Mar. Geol. 160, 183–196.
Li, J.F., Shi, W.R., Shen, H.T., 1994. Sediment properties and tranportation in the turbidity maximum in Changjiang estuary. Geophys. Res. 13 (1), 51–59 (in Chinese with English abstract).
Maloney, J.M., Bentley, S.J., Xu, K.H., Obelcz, J., Georgiou, I.Y., Jafari, N.H., Miner, M.D., 2019. Mass wasting on the Mississippi River subaqueous delta. Earth Sci. Rev. 200, 103001. https://doi.org/10.1016/j.earscirev.2019.103001.
Nienhuis, J.H., Ashton, A.D., Edmonds, D.A., Hoitink, A.J.F., Kettner, A.J., Rowland, J.C., Törnqvist, T.E., 2020. Global-scale human impact on delta morphology has led to net

land area gain. Nature 577 (7791), 514–518.
Qin, Y.S., Zhao, Y.Y., Chen, L.R., Zhao, S.L., 1987. Geology of the East China Sea. Science Press, Beijing.
Shen, H.T., 1985. Age and formation of the relict deposition on inner shelf of the East China Sea. Acta Oceanol. Sin. 7 (1), 67–77 (in Chinese with English abstract).
Shen, H.T., 2001. Material Flux of the Changjiang Estuary. Ocean Press, Beijing (in Chinese).
Shen, H.T., Zhu, H.F., Mao, Z.C., 1986. Circulation of the Changjiang River estuary and its effect on the transport of suspended sediment. Oceanol. Et Limnol. Sin. 17 (1), 26–35 (in Chinese with English abstract).
Shen, H.T., Mao, Z.C., Zhu, J.R., 2003. Saltwater Intrusion in the Changjiang Estuary. Ocean Press, Beijing (in Chinese).
Stanley, D.J., Warne, A.G., 1994. Worldwide initiation of Holocene marine deltas by deceleration of sea-level rise. Science 265, 228–231.
Stuiver, M., Reimer, P.J., Reimer, R., 2015. CALIB: Radiocarbon Calibration. (http://calib. qub.ac.uk/calib/ (September 2015)).
Sun, Y., Gao, S., Li, J., 2003. Preliminary analysis of grain-size populations with environmentally sensitive terrigenous components in marginal sea setting. Chin. Sci. Bull. 48 (2), 182–187.
Syvitski, J.P.M., Kettner, A.J., Overeem, I., Hutton, E.W.H., Hannon, M.T., Brakenridge, G.R., Day, J., Vorosmarty, C., Saito, Y., Giosan, L., Nicholls, R.J., 2009. Sinking deltas due to human activities. Nat. Geosci. 2, 681–686.
Wang, H., Yang, Z., Wang, Y., Saito, Y., Liu, J.P., 2008. Reconstruction of sediment flux from the Changjiang (Yangtze River) to the sea since the 1860s. J. Hydrol. 349, 318–332.
Wang, X., Shi, X.F., Wang, G.Q., Qiao, S.Q., Liu, T., 2013. Sedimentation rates and its indication to distribution of Yangtze sediment supply around the Yangtze (Changjiang) River estuary and its adjacent area, China. Edit. Commit. Earth Sci. 38 (4), 763–775.
Wang, Z.H., Saito, Y., Zhan, Q., Nian, X.M., Pan, D.D., Wang, L., Chen, T., Xie, J.L., Li, Xiao, Jiang, X.Z., 2018. Three-dimensional evolution of the Yangtze River mouth, China during the Holocene: Impacts of sea level, climate and human activity. Earth-Sci. Rev. 185, 938–955.
Wei, T.Y., Chen, Z.Y., Duan, L.Y., Gu, J.W., Saito, Y., Zhang, W.G., Wang, Y.H., Kanai, Y., 2007. Sedimentation rates in relation to sedimentary processes of the Yangtze Estuary, China. Estuar. Coast. Shelf 71, 37–46.
Xiao, S.B., Li, A.C., Liu, J.P., Chen, M.H., Xie, Q., Jiang, F.Q., Li, T.G., Xiang, R., Chen, Z., 2006. Coherence between solar activity and the East Asian winter monsoon variability in the past 8000 years from Yangtze River-derived mud in the East China Sea. Palaeogeogr. Palaeoclimatol. Palaeoecol. 237 (2–4), 293–304.
Xie, W.J., Gao, S., Yang, Y., 2012. Spatial distributions of grain size and 210Pb characteristics over the Chang Jiang subaqueous delta. Q. Sci. 32 (06), 1121–1131.
Luo, X.X., Yang, S.L., Zhang, J., 2012. The impact of the Three Gorges Dam on the downstream distribution and texture of sediments along the middle and lower Yangtze River (Changjiang) and its estuary, and subsequent sediment dispersal in the East China Sea. Geomorphology 179, 126–140.
Yang, S.L., Belkin, I.M., Belkina, A.I., Zhao, Q.Y., Zhu, J., Ding, P.X., 2003. Delta response to decline in sediment supply from the Yangtze River: evidence of the recent four decades and expectations for the next half-century. Estuar. Coast. Shelf Sci. 57 (4), 689–699.
Yang, S.L., Milliman, J.D., Li, P., Xu, K., 2011. 50,000 dams later: erosion of the Yangtze River and its delta. Glob. Planet. Chang. 75 (1), 14–20. https://doi.org/10.1016/j.gloplacha.2010.09.006.
Yang, S.L., Milliman, J.D., Xu, K.H., Deng, B., Zhang, X.Y., Luo, X.X., 2014. Downstream sedimentary and geomorphic impacts of the Three Gorges Dam on the Yangtze River. Earth Sci. Rev. 138, 469–486. https://doi.org/10.1016/j.earscirew.2014.07.006.
Luo, X.X., Yang, S.L., Wang, R.S., Zhang, C.Y., Li, P., 2017. New evidence of Yangtze delta recession after closing of the Three Gorges Dam. Sci. Rep. 7.
Yoneda, M., Uno, H., Shibata, Y., Suzuki, R., Kumamoto, Y., Yoshida, K., Sasaki, T., Suzuki, A., Kawahata, H., 2007. Radiocarbon marine reservoir ages in the western Pacific estimated by pre-bomb molluscan shells. Nucl. Instr. Methods Phys. Res. B259, 432–437.
Yun, C.X., 2010. Illustrations of the Changjiang Estuary Evolution. Ocean Press, Beijing.
Zhan, Q., Wang, Z.H., Chen, Y., Zhao, B.C., 2016. Grain size of recent sediments in Yangtze River subaqueous delta and its response to sediments supply decline. Geol. Bull. China 35 (10), 1715–1723 (in Chinese with English abstract).
Zhang, X.D., Zhai, S.K., Xu, S.M., 2007. The grain size fractions distribution characteristics and their significance of the surface sediments on the adjacent sea area off the Changjiang Estuary. Period. Ocean Univ. China 37 (02), 328–334 (in Chinese with English abstract).
Zhang, R., Pang, S.M., Wang, Y.P., Gao, J.H., 2008a. Characteritics of 137Cs geochemical distribution in the subaqueous delta of the Chang Jiang estuary. Q. Sci. 26 (04), 629–639.
Zhang, R., Wang, Y.P., Gao, J.H., Pan, S.M., Zhang, Z.L., 2008b. The vertical sedimentary structure and its implications for environmental evolutions in the Changjiang Estuary in China. Acta Oceanol. Sin. 30 (2), 80–91 (in Chinese with English abstract).
Zhang, M., Ian, T., Zhou, Y.X., Wang, L.H., Dai, Z.J., 2019. An examination of estuary stability in response to human interventions in the South Branch of the Yangtze (Changjiang) estuary, China. Estuar. Coast. Shelf Sci. 228, 1–14.
Zong, Y., Chen, Z., Innes, J.B., Chen, C., Wang, Z., Wang, H., 2007. Fire and flood management of coastal swamp enabled first rice paddy cultivation in east China. Nature 449, 459–462. https://doi.org/10.1038/nature06135.